Time-frequency based feature extraction for the analysis of vibroarthographic signals

Article *in* Computers & Electrical Engineering · March 2018

DOI: 10.1016/j.compeleceng.2018.02.046

4 authors:

Saif Nalband
DY Patil International University
10 PUBLICATIONS **79** CITATIONS
SEE PROFILE

Valliappan Ca
Indian Institute of Science
9 PUBLICATIONS **29** CITATIONS
SEE PROFILE

A Amalin Prince
BITS Pilani, K K Birla Goa
34 PUBLICATIONS **142** CITATIONS
SEE PROFILE

Anita Agrawal
BITS Pilani, K K Birla Goa
24 PUBLICATIONS **134** CITATIONS
SEE PROFILE

Computers and Electrical Engineering 000 (2018) 1–12

Contents lists available at ScienceDirect

Computers and Electrical Engineering

journal homepage: www.elsevier.com/locate/compeleceng

Time-frequency based feature extraction for the analysis of vibroarthographic signals☆

Saif Nalband, C.A. Valliappan, A. Amalin Prince*, Anita Agrawal

Department of Electrical and Electronics Engineering, Birla Institute of Technology and Science, Pilani, KK Birla Goa Campus, Goa 403726, India

ARTICLE INFO

Article history:
Received 8 September 2017
Revised 27 February 2018
Accepted 28 February 2018
Available online xxx

Keywords:
Knee-joint disorders
Vibroarthographic signals
Time-frequency
LS-SVM
Biomedical signal processing

ABSTRACT

In this study, we propose to develop a computer-aided diagnostic (CAD) system based on time-frequency analysis for the diagnosis of knee-joint disorders. Two methodologies based on nonstationary signal processing techniques have been proposed. We propose to use smoothed pseudo Wigner–Ville distribution (SPWVD) and a modified version of Hilbert–Huang transform (HHT) for the analysis of vibroarthographic (VAG) signals. Traditional HHT consists of empirical mode decomposition (EMD) for computing intrinsic mode functions (IMFs) and Hilbert transform (HT). But we propose to use complete ensemble empirical mode decomposition with adaptive noise (CEEMDAN) for computing IMFs. The time-frequency representation of the proposed methods is considered as a time-frequency image. Statistical features such as mean, standard deviation, skewness and kurtosis are extracted. A pattern classification is carried out using Least square support vector machine (LS-SVM) to compare performance. Results concluded that highest classification accuracy of 88.76% was obtained by features extracted from CEEMDAN-HHT.

1. Introduction

The early diagnosis of knee joint disorders plays a vital role considering the complexity of the knee joint structure. Presently, invasive and non-invasive methods are available for early diagnostic of knee joint disorders. An invasive method such as arthroscopy is not only expensive but also quite prone to infection and is not suitable for a daily routine diagnostic [1]. Computer tomography(CT), magnetic resonance imaging (MRI), X-rays etc. are some of the most common non-invasive methods. These diagnostics methods provide only static information since they are image based diagnosis and thereby do not provide the changing characteristics of knee joints. Additionally, these methods are expensive and cannot be used on a regular basis. Thus, an alternative diagnostic system that is non-invasive, cost effective and configurable with CAD could provide an early diagnostic system for knee joint disorders. Vibroarthrography (VAG) signals along with CAD could provide these attributes for diagnosing knee joint disorders [2].

VAG signals are the auditory sounds or the vibrations emitted from the mid patella during the active movements of the leg. VAG signals are multicomponent, nonlinear and nonstationary in nature [2]. Hence, the analysis of VAG signals with traditional digital signal processing methods would not be preferred. Time-frequency analysis provides an effective tool for understanding the nonstationary and nonlinear nature of signal. It has been studied in the analysis of biomedical signals

☆ Reviews processed and recommended for publication to the Editor-in-Chief by Area Editor Dr. E. Cabal-Yepez.

* Corresponding author.
E-mail address: amalinprince@gmail.com (A.A. Prince).

https://doi.org/10.1016/j.compeleceng.2018.02.046
0045-7906/

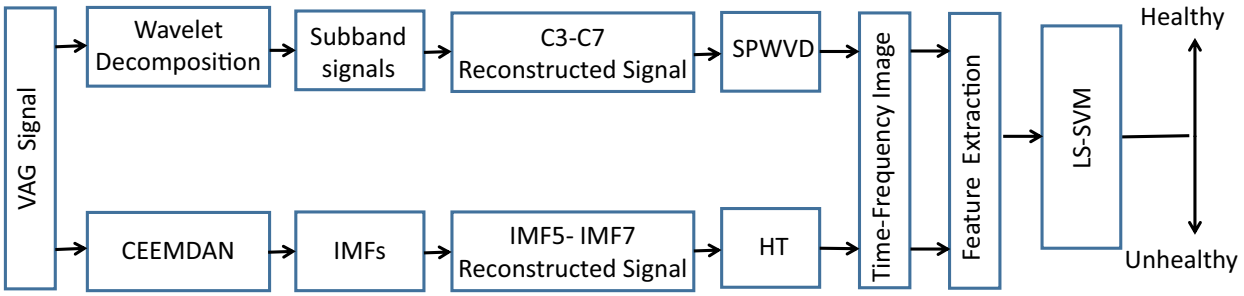

Fig. 1. Block diagram of proposed methodology.

List of abbreviation

ACC	Accuracy
BPNN	Back Propagation Neural Network
CAD	Computer-Aided Diagnostic
CEEMDAN	Complete Ensemble Empirical Mode Decomposition with Added Noise
EEMD	Ensemble Empirical Mode Decomposition
EMD	Empirical Mode Decomposition
FDR	False Discovery Detection
HHT	Hilbert Huang Transform
IMF	Intrinsic Mode Functions
LDA	Linear Discriminant Analysis
LS-SVM	Least Square Support Vector Machine
MCC	Matthews Correlation Coefficient
MLD	Modified Local Discriminant
MP	Matching Pursuit
NPV	Negative Predictive Value
PPV	Positive Predictive Value
AUC-ROC	Area Under the Receiver Operating Characteristic
SD	Standard Deviation
SEN	Sensitivity
SPE	Specificity
SPWVD	Smooth Pseudo Wigner Ville Distribution
TFD	Time Frequency Distribution
VAG	Vibroarthrography
WPD	Wavelet Packet Decomposition

such as ECG, EEG, EMG etc. [3,4]. Time-frequency analysis of VAG signals has been also carried by various researchers. Krishna et al. applied time-frequency distribution (TFD) by matching pursuit (MP) decomposition algorithm [2,5]. Umapathy et al. computed TFD by using modified local discriminant [6]. Chen et al. have used traditional Hilbert Huang transform (HHT) for VAG signals [7]. The time-frequency analysis of knee joint has been carried out in relation to specific age group by Baczkowicz et al. [8]. The discrete Fourier transform was applied to segmented VAG signals for obtaining short time spectrum. From literature survey, it has been concluded that, most of the TFD of VAG signals were quite restrictive to classical signal processing techniques. Therefore, further analysis of VAG signals using TFD could be carried out using advance time-frequency techniques.

VAG signals are nonlinear, nonstationary and multicomponent in nature. Considering these characteristics, nonstationary signal processing techniques have been carried out. Two approaches based on linear and nonlinear signal processing techniques have been proposed. Fig. 1 shows the block diagram of the proposed methodology using time-frequency analysis.

We propose to use nonstationary linear signal processing technique namely wavelet packet decomposition (WPD) [9] and nonstationary nonlinear signal processing technique namely complete ensemble empirical mode decomposition with adaptive noise (CEEMDAN) [10]. These techniques are used as preprocessing techniques for the analysis of VAG signals.

In the first method, we proposed to use smooth pseudo Wigner–Ville distribution (SPWVD) for obtaining the time-frequency distribution (TFD) [11]. SPWVD overcomes the problem of interference of cross terms in Wigner–Ville distribution. We propose to use WPD to decompose the VAG signal into subband signals of different frequencies. The VAG signals were reconstructed from significant subband signals from WPD [12]. TFD of reconstructed VAG is obtained by using SPWVD and

Please cite this article as: S. Nalband et al., Time-frequency based feature extraction for the analysis of vibroarthographic signals, Computers and Electrical Engineering (2018), https://doi.org/10.1016/j.compeleceng.2018.02.046

this TFD is considered as the time-frequency image. Thereby the statistical features such as mean, standard deviation, skewness and kurtosis are extracted. This methodology is based on the nonstationary linear signal processing technique.

In the second approach, we proposed to use a modified version of Hilbert–Huang Transform (HHT) known as CEEMDAN-HHT. Traditional HHT consists of two parts: 1) Empirical Mode Decomposition (EMD) 2) Hilbert transform (HT) [13]. HHT has been successfully applied in the various applications related to geophysical studies, biomedical studies, vibration fault tolerance etc. [14]. EMD decomposes the signal into a number of intrinsic mode functions (IMF). But "mode mixing" is one of the major drawbacks of EMD. In mode mixing, a single IMF consists of signals having different scales [15]. This may lead to serious aliasing effects in time-frequency distribution and the resultant IMFs may lose their physical significance. To overcome this drawback "ensemble empirical mode decomposition" (EEMD) was proposed [15] and has been used for analysis of biomedical signals such as EEG, ECG etc. [16,17]. But, EEMD has a significant signal reconstruct error and does not provide a fixed number of IMFs. Thus, to overcome these drawbacks, we propose to use complete ensemble empirical mode decomposition with adaptive noise (CEEMDAN) for obtaining IMFs [10].

The VAG signal is decomposed into IMFs by CEEMDAN [18]. The VAG signal is reconstructed by dominant IMFs and TFD is obtained by applying Hilbert transform (HT). This TFD is considered as time-frequency image and statistical features consisting of mean, standard deviation, skewness and kurtosis are extracted from time-frequency image. This methodology is based on nonstationary nonlinear signal processing technique.

The extracted features obtained by using SPWVD and CEEMDAN-HHT are given as input to LS-SVM (as a classifier) and their performance is evaluated. Hence, a comparative study of different methodologies (nonstationary linear signal processing technique and nonstationary nonlinear signal processing technique) has been carried out and their performance have been compared.

The paper has been organized into the following sections. Section 2 covers a brief theoretical background of the proposed work. The results and discussion of the proposed work have been explained in Section 3. Finally, Section 4 summarises with the conclusion of our proposed study.

2. Methods

2.1. Wavelet packet decomposition (WPD)

The WPD algorithm disintegrates a given signal into detail coefficients and approximation to derive at the first stage of decomposition [9]. Thus, these approximation coefficients are further disintegrated into approximation and coefficients in successive stages. Hence the signal breaks down like a tree. At each stage approximation coefficients belong to a particular frequency. In the present study, we have used 4th (db4) order wavelet of debaucheries family for the decomposition of the signal. We have taken 10 levels of decomposition to get 11 detail coefficients and an approximation coefficient. WPD has been widely used in the analysis of biomedical signals such as EEG, EMG and VAG etc. [12,19].

2.2. SPWVD

Wigner–Ville distribution (WVD) is nonstationary time-frequency analysis which distributes the energy of the signal along the variables time and frequency [20]. Initially, it was introduced in the domain of quantum mechanics as Wigner distribution but later it was used in the framework of signal analysis as Wigner–Ville distribution. Moreover, WVD has better theoretical properties, but it has a major drawback as it produces cross term between components of multi-component signals. It means that there are additional components of signals present in the signal. In order to remove this, a separable smoothing window is introduced which is independent of time and frequency and it is called as smooth pseudo Wigner–Ville distribution [11]. Therefore, the time-frequency resolution can be controlled independently.

2.3. Hilbert Huang transform

The traditional HHT uses the EMD method to decompose the signal into intrinsic mode functions (IMF) [13]. EMD was specifically developed for time-frequency analysis of nonlinear and nonstationary signals. CEEMDAN has been proposed by Colominas et al. for computing IMFs [10]. Therefore in this study, we propose to use CEEMDAN for computing IMFs in the analysis of VAG signal.

2.3.1. CEEMDAN

Let E_k be the function which generates the *kth* mode/IMF from the EMD method as shown $E(s) = x - M(s)$ where '*s*' is the input signal and $M(.)$ is function that outputs local mean of the input signal. The 1st mode/IMF E_1 is defined as follows

$$E_1(s) = s - M(s) \tag{1}$$

here '*s*' denotes the input signal $E_1(s)$ provides the 1st decomposition by EMD. The steps for CEEMDAN are as follows

1. Initially, set of ensemble denoted as $s^{(i)}$ is computed with equation below

$$s^{(i)} = s + \beta_0 E_1(w^{(i)}). \tag{2}$$

Please cite this article as: S. Nalband et al., Time-frequency based feature extraction for the analysis of vibroarthographic signals, Computers and Electrical Engineering (2018), https://doi.org/10.1016/j.compeleceng.2018.02.046

where $w^{(i)}$ is white noise with zero mean and unit variance and $i \in (1, 2, \ldots I)$ is the ensemble number. Here β_0 is positive constants and in general $(\beta_{k-1} > 0)$, where k indicates the mode number.

2. The local of mean for *'I'* realization is computed by traditional EMD method i.e. $M(.)$ for the set of ensembles to get the 1st residue as shown in the equation

$$r_1 = \langle M(s^{(i)}) \rangle \tag{3}$$

Here $\langle . \rangle$ performs the averaging operation over all the $i \in (1, 2, \ldots, I)$.

3. The above computed residue r_1 is subtracted from the signal *'s'* to derive the first mode C_1 as shown in the equation

$$C_1 = s - r_1 \tag{4}$$

4. Now we consider residue r_1 as the base signal to compute the 2nd residue as an average of the local means of $r_1 + \beta_1 E_2(w^{(i)})$ **similar to equation in step 1** and this residue defines the 2nd mode C_2 as:

$$C_2 = r_1 - \langle M(r_1 + \beta_1 E_2(w^{(i)})) \rangle \tag{5}$$

5. From the above steps we can generalise that the *kth* residue is given by .

$$r_k = \langle M(r_{k-1} + \beta_{k-1} E_k(w^{(i)})) \rangle \tag{6}$$

6. The *kth* mode is calculated as

$$C_k = r_{k-1} - r_k \tag{7}$$

Repeat step 5 and 6 for the next mode until the residue r_k cannot be further decomposed by EMD.

Here *'I'* = ensemble number and *'w'* = Gaussian white noise. For obtaining a desirable SNR between the added Gaussian noise and the residue, the constants $\beta_k = \epsilon_k . std(r_k)$ are set appropriately. The value of β has been set in such a way that ϵ_0 is the reciprocal of SNR between the input signal and the added Gaussian white noise, i.e in term is standard deviation (SD).

$$\beta_0 = \frac{\epsilon_0 * SD(s)}{SD(E_1(w^{(i)}))} \tag{8}$$

There are two approaches for setting the stopping criteria. First by a fix number of shifting iteration and second based on energy parameters. In this work, the parameters for CEEMDAN were selected based on following measures.

(a) 5000 has been set as the number of shifting iteration.
(b) *'I'* is the ensemble number which has been set as 100.
(c) The added noise has been set as 0.2 X standard deviation (SD) of raw VAG signal.

2.3.2. Hilbert transform

In order to obtain the analytical signal $z(t)$, Hilbert transform is applied.

$$z(t) = s(t) + j * h(t) \tag{9}$$

where $s(t)$ is input signal and $h(t)$ Hilbert transform of input signal which is defined as

$$h(t) = \frac{1}{\pi} P \int_{-\infty}^{\infty} \frac{s(\tau)}{t - \tau} d\tau \tag{10}$$

Cauchy principal value for singular integral is defined as P.

2.4. Feature extraction

The time-frequency representation using SPWVD and CEEMDAN-HHT is considered as a time-frequency image of the signal and features are extracted [21]. The pixel intensity is used as the measure of calculated features. Each pixel corresponds to a particular time and frequency which represents the power of the signal at any instance of frequency. We extract statistical features such as mean, standard deviation, skewness and kurtosis from all the pixel intensity corresponding to each time-frequency image. Hence, from these statistical value we can get an overview of the essential information as attributes of the signal.

2.5. Least square-support vector machine

LS-SVM is supervised learning method for data analysis and pattern classification. It is an upgraded version of support vector machine [22]. In LS-SVM, the solution is obtained by solving linear equation instead of complex quadratic programing. The advantage of using LS-SVM over the standard SVM is the learning efficiency due to the similar linear equations.

Please cite this article as: S. Nalband et al., Time-frequency based feature extraction for the analysis of vibroarthographic signals, Computers and Electrical Engineering (2018), https://doi.org/10.1016/j.compeleceng.2018.02.046

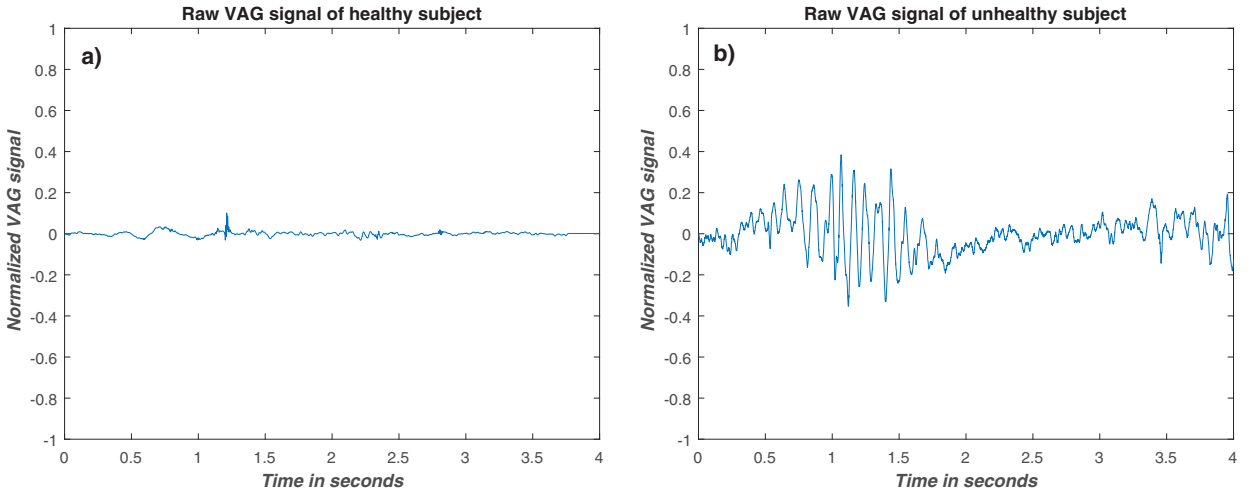

Fig. 2. VAG signal of a healthy and unhealthy person.

3. Results and discussion

3.1. Experimental dataset

The set up for data/signal acquisition of VAG signals was accomplished at the University of Calgary in Canada by a research group lead by Rangayyan [2]. The experiment protocol was given ethical clearance by the University of Calgary. The experiment consisted of 89 subjects (51 healthy subjects and 38 unhealthy subjects). Prior to experiment, these subjects were consulted and examined by a physician. The healthy subjects did not suffered from any knee joint diseases while unhealthy subjects suffered from various kinds of knee joint diseases. More details regarding the acquisition can be refereed to work described in [5]. Fig. 2(a) and (b) represents a sample of VAG signal of a healthy and unhealthy subject respectively.

3.2. Preprocessing

From Fig. 2, it can be observed that raw VAG signals contain baseline wanders and other interference of noises. A double cascaded moving average filter is applied on raw VAG signals to remove these artefacts [23]. The proposed work consisting of preprocessing, feature extraction and classification has been carried out in MATLAB 2015b. After filtering, the VAG signals are decomposed into subband signals and IMFs using WPD and CEEMDAN respectively.

Since the sampling rate of VAG is 2k, the frequency available would be 1 Khz. Hence, VAG signals are decomposed into 11 levels of subband signals (*C1, C2, C3, C4, C5, C6, C7, C8, C9, C10, b10*) and each subband signals consists of particular frequency [12]. Fig. 3(a) and (b) represents the subband signals obtained from WPD of healthy and unhealthy respectively.

Similarly, Fig. 4 represents the decomposed signal obtained from CEEMDAN. Fig. 4(a) and (b) shows the IMFs obtained using CEEMDAN. From figure, it can be observed that different dynamics involved in VAG signals are observed in different IMFs for healthy and unhealthy subject respectively. High frequency oscillation is observed in IMF1-IMF3 and low frequency oscillation can be seen in IMF4-IMF10. As observed, flat envelopes can be seen in IMF1 and IMF2 for both cases and can be discarded for the study since it does not signify any pathological condition.

3.3. Feature extraction

VAG signals were reconstructed from the subband signals. From Fig. 3, the subband signals *C1, C2, C8, C9 and C10* were ignored and were not considered for the study. *C8, C9 and C10* represented artefacts, while the subband signals *C1 and C2* indicated the presence of high-frequency components. VAG signal was reconstructed using subband signals (*C3, C4, C5, C6 and C7*) and is shown in Fig. 5(a) and (b). Fig. 5(c) and (d) represents the time-frequency representation using SPWVD and this is considered as time-frequency image. Hence, attributes such as mean, standard deviation, skewness and kurtosis are computed from time-frequency image and this has been carried for 89 samples of VAG signals.

Identifying the correct IMFs for VAG signal is carried out by computing detrended fluctuation analysis (DFA). The DFA computes the correlation properties of IMFs. The fractal scaling index (α) obtained from DFA helps in identifying the correct IMFs. The α value of the IMFs in the range between ($0 < \alpha < 0.5$) and IMF9-IMF10 (low frequency IMFs) have been eliminated as per the study concluded by Wu [24]. Hence, from the computed α value of IMF5, IMF6 and IMF7 (1.35, 1.64 and 1.83) are treated as correct IMFs of VAG signal. The VAG signal is regenerated by summation of correct IMFs and is shown in Fig. 6(a) and (b) for healthy and unhealthy VAG signal respectively. Fig. 6(c) and (d) represents the time-frequency

Please cite this article as: S. Nalband et al., Time-frequency based feature extraction for the analysis of vibroarthographic signals, Computers and Electrical Engineering (2018), https://doi.org/10.1016/j.compeleceng.2018.02.046

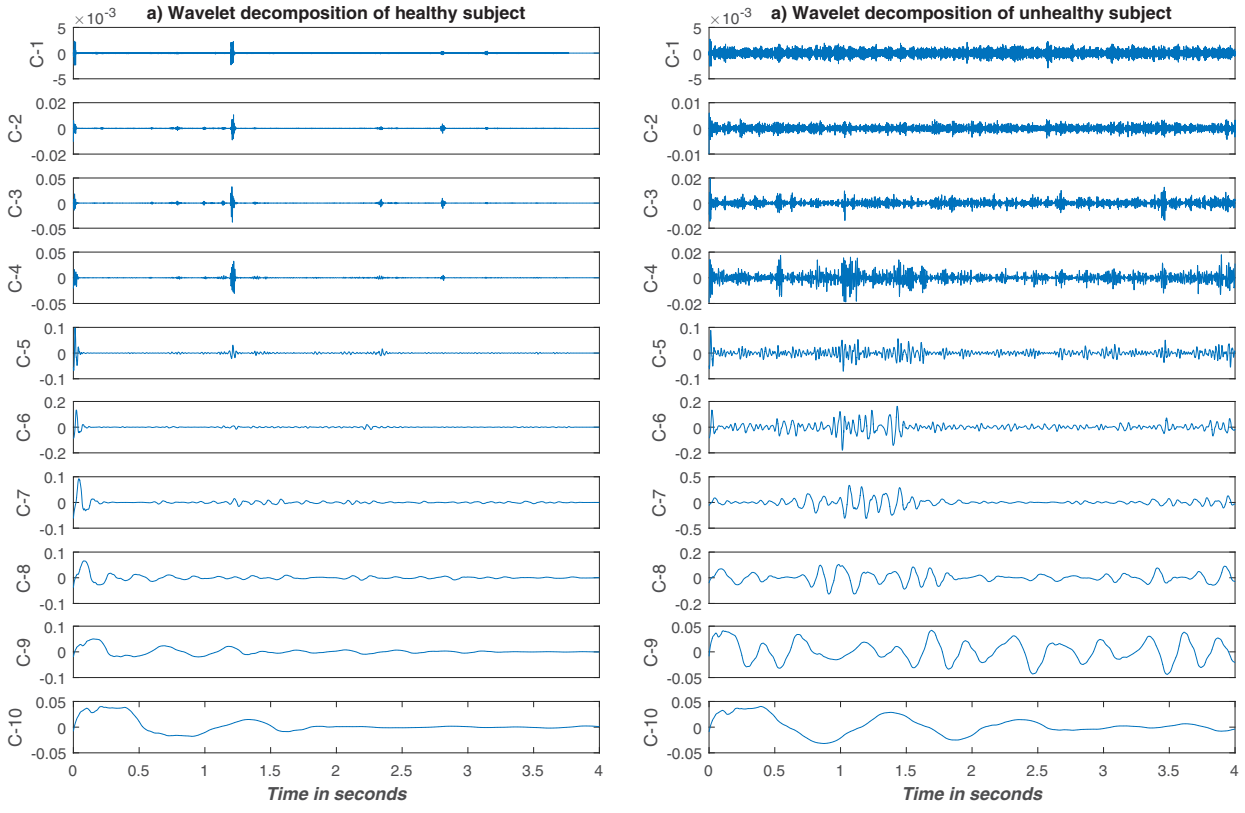

Fig. 3. Wavelet packet decomposition of VAG signal for a healthy and unhealthy subject.

Table 1
Statistical measures of extracted features using SPWVD and CEEMDAN-HHT.

class	Normal	Abnormal	
Features	Mean ± SD	Mean ± SD	*p-value*
SPWVD			
Mean	0.3461 ± 0.0662	0.3330 ± 0.0766	0.3237
Standard	1.6886 ± 0.3238	1.6224 ± 0.3766	0.3136
skewness	6.7910 ± 0.0900	6.8137 ± 0.1127	0.2663
Kurtosis	52.7752 ± 2.1699	53.4333 ± 2.6143	0.2050
CEEMDAN-HHT			
Mean	0.3587 ± 0.0769	0.3373 ± 0.0670	0.1167
STD	1.7578 ± 0.3705	1.6550 ± 0.3224	0.1293
skewness	7.0215 ± 0.3311	7.1490 ± 0.3979	0.0629
Kurtosis	58.7469 ± 8.8681	62.2163 ± 10.6879	0.0559

representation of the reconstructed VAG signals. This representation is considered as time-frequency image and individual attributes such as mean, standard deviation, skewness and kurtosis are computed. From Fig. 6(a) and (b) it can be observed that the variation of frequency is highly variant in case of unhealthy VAG signals as compared to healthy VAG signal.

From Figs. 5 and 6, it can be inferred that the unhealthy VAG signal provided larger variation as compared to healthy subjects. The cause of this large variation might be due to wear and tear of the muscle tissues associated with the knee joint. As a result, it does not allow free leg movements in performing extension and flexion. While comparing the Figs. 5 and 6, it can be observed that the time-frequency image of CEEMDAN-HHT is sharper than time-frequency image of SPWVD. It also provides a better variation, especially in the case of the unhealthy VAG signal.

The Kruskal–Wallis, a statistical test was performed on the features extracted from time-frequency image. The *p*-values signify the discrimination between the two distributions. The return *p*-values signify that, lower the *p*-value, the better is the feature discrimination between healthy and unhealthy groups. Table 1 refer the mean, standard deviation and *p*-value computed for extracted features (mean, standard deviation, skewness and kurtosis) from SPWVD and CEEMDAN-HHT. Fig. 7 provides the box plots for extracted features for SPWVD and CEEMDAN-HHT.

Please cite this article as: S. Nalband et al., Time-frequency based feature extraction for the analysis of vibroarthographic signals, Computers and Electrical Engineering (2018), https://doi.org/10.1016/j.compeleceng.2018.02.046

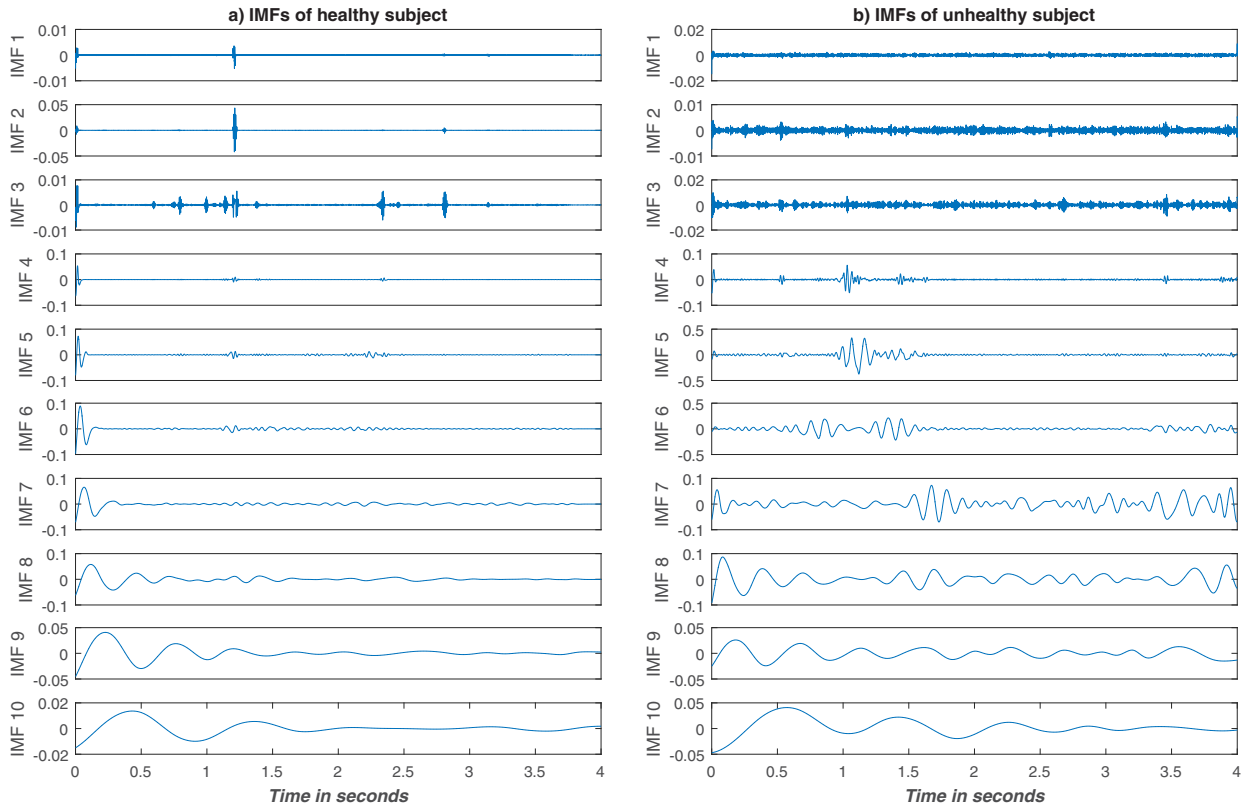

Fig. 4. IMFs of VAG signals obtained using CEEMDAN for a healthy and unhealthy subject.

Table 2
Classification of features extracted using SPWVD by LS-SVM.

	Vector	Mean	SD	Skewness	Kurtosis
ACC	0.7753	0.7865	0.6667	0.7416	0.6180
SEN	0.9091	0.8800	0.8000	0.7586	0.6429
SPE	0.7313	0.7500	0.6389	0.7333	0.6133
PPV	0.5263	0.5789	0.3158	0.5789	0.2368
NPV	0.9608	0.9412	0.9388	0.8627	0.9020
MCC	0.5585	0.5724	0.3343	0.4661	0.1886
FDR	0.4737	0.4211	0.6842	0.4211	0.7632
AUC-ROC	0.7699 ± 0.0573	0.8945 ± 0.0622	0.7281 ± 0.0593	0.7384 ± 0.0620	0.6744 ± 0.0594

From Table 1 and Fig. 7, it can be observe that there is clear distinction between healthy and unhealthy group of VAG signals. Moreover, it can be concluded that features extracted from unhealthy group provided huge variation as compared to healthy group. The cause of this large variation might be due to wear and tear of the muscle tissues associated with the knee joint which restricts the free leg movements in performing extension and flexion. Hence, the statistical analysis provided a significant difference between the groups and these extracted features are given as input to classifier in building classification model.

3.4. Classification

The extracted features from SPWVD, and CEEMDAN-HHT are given as inputs to LS-SVM. In our study, we have used radial basis function (RBF) as kernel function. The kernel parameters were evaluated using the “gridsearch” algorithm. Regularization constant was selected appropriately for avoiding over-fitting and 10 cross validation was performed. The performance of proposed system was evaluated based on parameters such as sensitivity (SEN), specificity(SPE), accuracy(ACC), Matthews correlation coefficient (MCC), false discovery detection rate (FDR), negative predictive value (NPV) and positive predictive value (PPV).

Tables 2 and 3 provides the classification performance of LS-SVM using features extracted from time-frequency image of SPWVD and CEEMDAN-HHT respectively. The classification performance has been evaluated with features given as individual

Please cite this article as: S. Nalband et al., Time-frequency based feature extraction for the analysis of vibroarthographic signals, Computers and Electrical Engineering (2018), https://doi.org/10.1016/j.compeleceng.2018.02.046

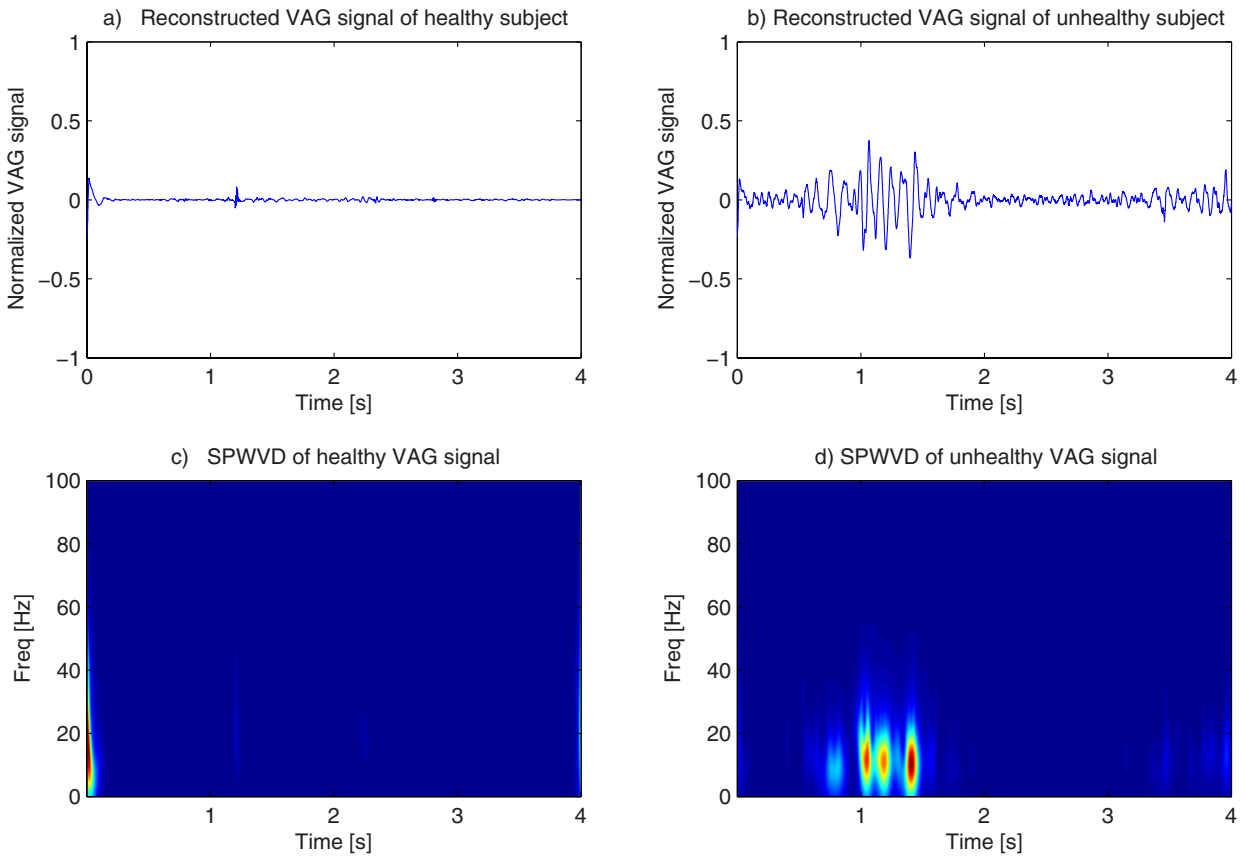

Fig. 5. The reconstructed VAG signal obtained from SPWVD (a) healthy subject and (b) unhealthy subject. Time-frequency representation of VAG signal c) healthy subject and d) unhealthy subject.

Table 3
Classification of features extracted using CEEMDAN-HHT by LS-SVM.

	Vector	Mean	SD	Skewness	Kurtosis
ACC	0.8202	0.8876	0.8764	0.7978	0.7865
SEN	0.8750	0.8333	0.9655	0.7500	0.7209
SPE	0.7895	0.9362	0.8333	0.8367	0.8478
PPV	0.7000	0.9211	0.7368	0.7895	0.8158
NPV	0.9184	0.8627	0.9804	0.8039	0.7647
MCC	0.6410	0.7766	0.7569	0.5901	0.5746
FDR	0.3000	0.0789	0.2632	0.2105	0.1842
AUC-ROC	0.8994 ± 0.0579	0.9383 ± 0.0615	0.9494 ± 0.0617	0.8127 ± 0.0617	0.8519 ± 0.0568

input and as a vector of all features (mean, standard deviation, skewness and kurtosis) to LS-SVM. The performance of features of CEEMDAN-HHT given as a vector provides an accuracy of 82.02% with a sensitivity of 87.50% and specificity of 78.95%. MCC is 0.6410 with low FDR of 0.3000 for a vector of features as observed in Table 3. But the highest classification accuracy has been obtained for the feature “mean” which gives an accuracy of 88.76% with a highest MCC value of 0.7766 and low FDR of 0.0789 using CEEMDAN-HHT (Table 3). The highest accuracy obtained using SPWVD gives 77.53% for a vector of all features, it is less than the accuracies obtained with the features extracted from CEEMDAN-HHT (ACC = 82.02% for a vector of features). As observed from the Tables 2 and 3, CEEMDAN-HHT provided better classification performance with respect to SPWVD. The other parameters of classification also inferred that the features extracted from CEEMDAN-HHT provided better pattern classification than SPWVD.

Graphical representation of classifier was evaluated using receiver operating characteristic (ROC). The area under the curve (AUC) provides the effectiveness of the classifier. The AUC-ROC plot for individual features and vector of features extracted from SPWVD and CEEMDAN-HHT are shown in Fig. 8 (a) and (b) respectively. The highest (AUC-ROC = 0.9383 ± 0.0615) is obtained for feature “mean” extracted from CEEMDAN-HHT. These parameters implied that using LS-SVM classi-

Please cite this article as: S. Nalband et al., Time-frequency based feature extraction for the analysis of vibroarthographic signals, Computers and Electrical Engineering (2018), https://doi.org/10.1016/j.compeleceng.2018.02.046

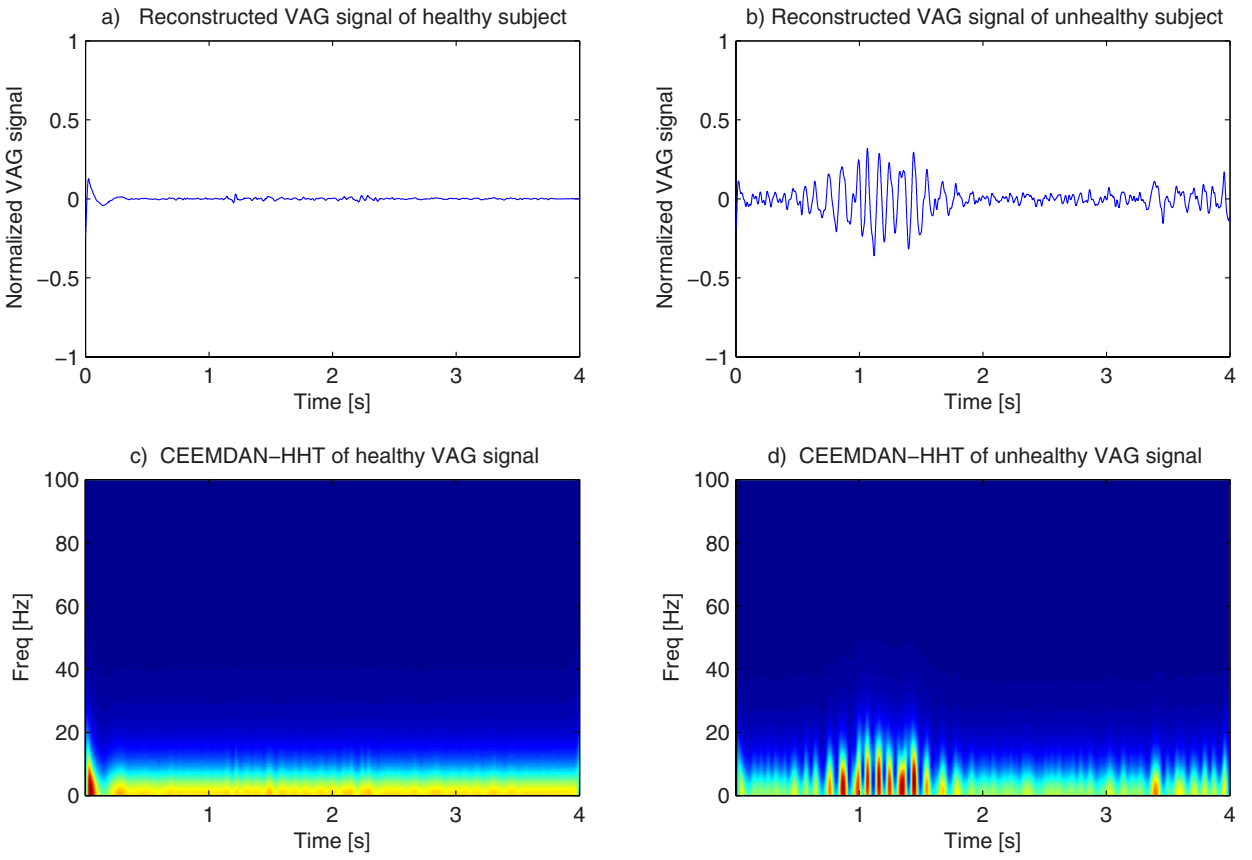

Fig. 6. The reconstructed VAG signal obtained from CEEMDAN (a) healthy subject and (b) unhealthy subject. Time-frequency representation of VAG signal (c) healthy subject and (d) unhealthy subject.

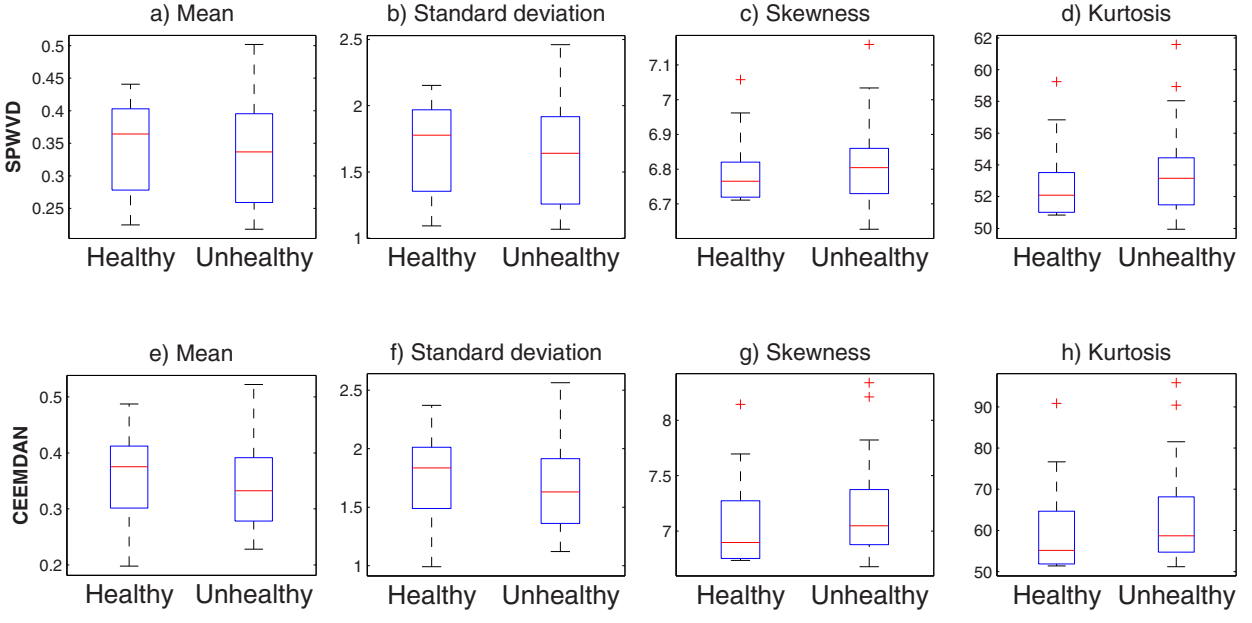

Fig. 7. Box plots for features extracted from SPWVD and CEEMDAN-HHT.

Please cite this article as: S. Nalband et al., Time-frequency based feature extraction for the analysis of vibroarthographic signals, Computers and Electrical Engineering (2018), https://doi.org/10.1016/j.compeleceng.2018.02.046

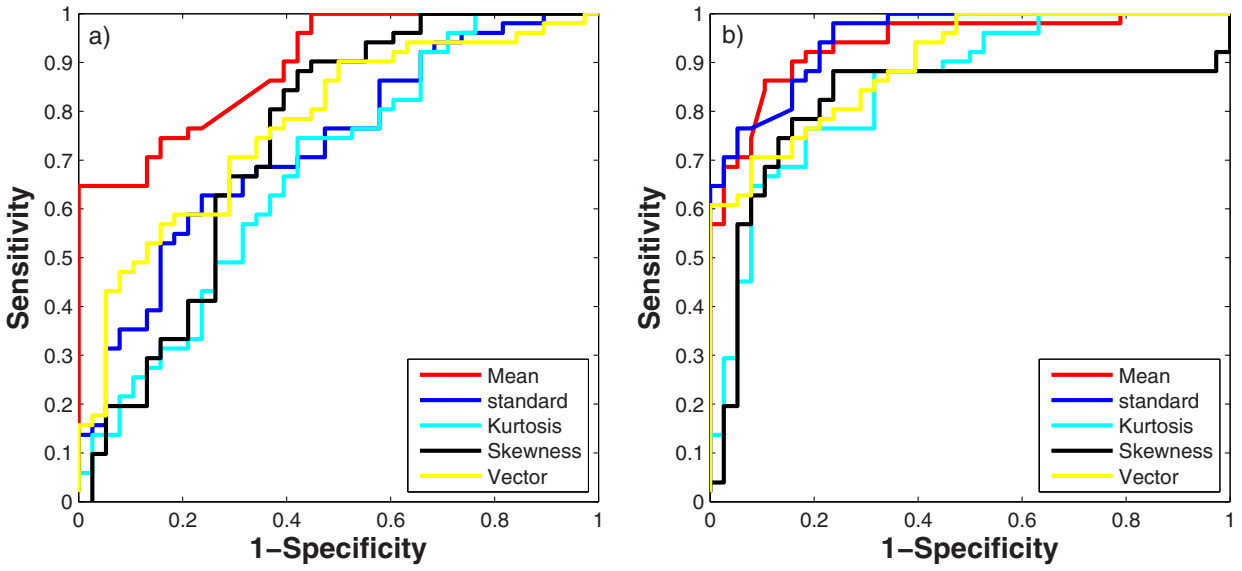

Fig. 8. Performance of ROC plot a) SPWVD and b) CEEMDAN-HHT.

Table 4
Comparison of the proposed methodology with the existing TFD.

Methodology	MP [2]	MP [5]	MLD [6]	EMD-HHT [7]	CEEMDAN
ACC	77.8	68.9	79.8	85.3	88.76
SEN	NA	NA	NA	NA	0.833
SPE	NA	NA	NA	NA	0.9362
MCC	NA	NA	NA	NA	0.7766
Classifier	DA	LR	LDA	NA	LS-SVM
No of samples	37	90	89	35	89

fier technique, a larger number of VAG signals were precisely categorized into healthy and unhealthy classes for features extracted from CEEMDAN-HHT.

Table 4 represents comparison of the proposed work with the existing work reported in the time-frequency analysis of VAG signals. Initial study carried out by Krishnan et al. consisted of 37 samples of VAG signals [2]. The time-frequency distribution was obtained by matching pursuit method (MP) method and it gave a classification accuracy of 77.8%. Krishnan et al. continued his work by constructing adaptive time-frequency distribution by minimizing the cross optimization of time-frequency distribution computed by the MP method [5]. The work consisted of 90 samples of VAG signals which gave a classification accuracy of 68.9% using logistic regression. Umapathy et al. further carried out the time-frequency analysis by computing TFD using modified local discriminant (MLD) [6]. It gave a classification accuracy of 79.8% using linear discriminant analysis. Chen et al. carried out the analysis using traditional HHT (using EMD for computing IMFs) which gave a classification accuracy of 85.3% [7]. Chen used different dataset which consisted of 35 (12 healthy subjects and 23 unhealthy subjects) samples of VAG signal. Different data acquisition system had been applied for acquiring VAG signals (different accelerometers sensor, DAQ board, sampling frequency). The dataset consisted of few samples of VAG signals and therefore, comparing the results of different dataset would not be ideal. From Table 4 it can be observed that, the proposed method of CEEMDAN-HHT performed better with respect to other methodologies. The proposed methodology (CEEMDAN-HHT) gives the highest classification accuracy of 88.76% using LS-SVM.

4. Conclusion

This study proposed a CAD system using time-frequency analysis of VAG signals. The analysis has been carried out using nonstationary signal processing techniques. Time-frequency based techniques namely, SPWVD and CEEMDAN-HHT has been investigated and their performances has been evaluated. The time-frequency representation of VAG signals has been considered as time-frequency image and statistical features based on image pixels were extracted. Results concluded that time-frequency technique using CEEMDAN-HHT provided a prominent distinction between the healthy and unhealthy group. Furthermore, the pattern classification results also concluded that CEEMDAN-HHT performed better with respect to SPWVD by giving the highest accuracy of 88.76%, AUC-ROC: 0.9383 $\pm$ 0.0615 and MCC of 0.7766 with low FDR of 0.0789. The proposed work provided a better methodology in analysing nonlinear, nonstationary and multicomponent VAG signals using

Please cite this article as: S. Nalband et al., Time-frequency based feature extraction for the analysis of vibroarthographic signals, Computers and Electrical Engineering (2018), https://doi.org/10.1016/j.compeleceng.2018.02.046

time-frequency techniques. Hence, a CAD system could be developed with proposed methodology for non-invasive diagnosis of knee joint disorders.

Acknowledgements

We are highly beholder to the research group of Rangaraj M. Rangayyan from University of Calgary, Canada for providing the permission to use their data set for our study.

References

[1] Thorlund JB, Juhl CB, Roos EM, Lohmander LS. Arthroscopic surgery for degenerative knee: systematic review and meta-analysis of benefits and harms. BMJ (Clinical research ed) 2015;350(11):h2747. doi:10.1136/bmj.h2747.
[2] Krishnan S, Rangayyan RM, Bell GGD, Frank CB. Time-frequency signal feature extraction and screening of knee joint vibroarthrographic signals using the matching pursuit method. In: Engineering in medicine and biology society, 1997. Proceedings of the 19th annual international conference of the IEEE, 3. IEEE; 1997. p. 1309–12.
[3] Lee J, McManus DD, Bourrell P, Sörnmo L, Chon KH. Atrial flutter and atrial tachycardia detection using Bayesian approach with high resolution time-frequency spectrum from ECG recordings. Biomed Signal Process Control 2013;8(6):992–9. doi:10.1016/j.bspc.2013.04.002.
[4] Subasi A, Kiymik MK. Muscle fatigue detection in EMG using time-frequency methods, ICA and neural networks. J Med Syst 2010;34(4):777–85. doi:10.1007/s10916-009-9292-7.
[5] Krishnan S, Rangayyan RM, Bell GD, Frank CB. Adaptive time-frequency analysis of knee joint vibroarthrographic signals for noninvasive screening of articular cartilage pathology. IEEE Trans Biomed Eng 2000;47(6):773–83. doi:10.1109/10.844228.
[6] Umapathy K, Krishnan S. Modified local discriminant bases algorithm and its application in analysis of human knee joint vibration signals. IEEE Trans Biomed Eng 2006;53(3):517–23. doi:10.1109/TBME.2005.869787.
[7] Chen J-C, Tung P-C, Huang S-F, Wu S-W, Lin S-L, Tu K-L. Extraction and screening of knee joint vibroarthrographic signals using the empirical mode decomposition method. Int J Innovative Comput Inf Control 2013;9(6):2689–700.
[8] Baczkowicz D, Majorczyk E, Krecisz K. Age-related impairment of quality of joint motion in vibroarthrographic signal analysis. Biomed Res Int 2015;2015. doi:10.1155/2015/591707.
[9] Mallat S. A wavelet tour of signal processing the sparse way. Academic press; 2008. 9780123743701.
[10] Colominas MA, Schlotthauer G, Torres ME. Improved complete ensemble EMD: a suitable tool for biomedical signal processing. Biomed Signal Process Control 2014;14(1):19–29. doi:10.1016/j.bspc.2014.06.009.
[11] Hlawatsch F, Manickam TG, Urbanke RL, Jones W. Smoothed pseudo-Wigner distribution, Choi-Williams distribution, and cone-kernel representation: Ambiguity-domain analysis and experimental comparison. Signal Process 1995;43(2):149–68. doi:10.1016/0165-1684(94)00150-X.
[12] Nalband S, Sundar A, Prince AA, Agarwal A. Feature selection and classification methodology for the detection of knee-joint disorders. Comput Methods Programs Biomed 2016;127:94–104.
[13] Huang NE, Shen Z, Long SR, Wu MC, Shih HH, Yen N-c, et al. The empirical mode decomposition and the hilbert spectrum for nonlinear and non-stationary time series analysis. R Soc London Proc Ser A 1996;454(1):903–95. doi:10.1098/rspa.1998.0193.
[14] Huang NE, Shen SSP. Hilbert-Huang transform and its applications, 5. World Scientific Publishing Co. Pte. Ltd.; 2014. ISBN 9789814508230. doi:10.1142/9789812703347.
[15] Zhaohua WU, Huang NE. Ensemble empirical mode decomposition: a noise-Assisted data analysis method. Adv Adapt Data Anal 2009;01(01):1–41. doi:10.1142/S1793536909000047.
[16] Patel R, Sengottuvel S, Janawadkar M, Gireesan K, Radhakrishnan T, Mariyappa N. Ocular artifact suppression from eeg using ensemble empirical mode decomposition with principal component analysis. Comput Electr Eng 2016;54:78–86. doi:10.1016/j.compeleceng.2015.08.019.
[17] Saini I, Singh D, Khosla A. Electrocardiogram beat classification using empirical mode decomposition and multiclass directed acyclic graph support vector machine. Comput Electr Eng 2014;40(5):1774–87. doi:10.1016/j.compeleceng.2014.04.004.
[18] Nalband S, Prince A, Agrawal A. Entropy-based feature extraction and classification of vibroarthographic signal using complete ensemble empirical mode decomposition with adaptive noise. IET Sci Measure Technol 2017. doi:10.1049/iet-smt.2017.0284.
[19] Chen LL, Zhang J, Zou JZ, Zhao CJ, Wang GS. A framework on wavelet-based nonlinear features and extreme learning machine for epileptic seizure detection. Biomed Signal Process Control 2014;10(1):1–10. doi:10.1016/j.bspc.2013.11.010.
[20] Ghofrani S, Ayatollahi a, Shamsollahi MB. Wigner ville distribution. Proc IEEE 1993;39(2). 2–2 http://www.ncbi.nlm.nih.gov/pubmed/20160789.
[21] Bajaj V, Pachori RB. Automatic classification of sleep stages based on the time-frequency image of EEG signals. Comput Methods Programs Biomed 2013;112(3):320–8. doi:10.1016/j.cmpb.2013.07.006.
[22] Vapnik V.N., Chervonenkis A.Y. On the uniform convergence of relative frequencies of events to their probabilities. 1971. doi:10.1137/1116025.
[23] Cai S, Wu Y, Xiang N, Zhong Z, He J, Shi L, et al. Detrending knee joint vibration signals with a cascade moving average filter. Proc Annu Int Conf IEEE Eng Med Biol Soc EMBS 2012:4357–60. doi:10.1109/EMBC.2012.6346931.
[24] Wu Y, Yang S, Zheng F, Cai S, Lu M, Wu M. Removal of artifacts in knee joint vibroarthrographic signals using ensemble empirical mode decomposition and detrended fluctuation analysis. Physiol Meas 2014;35(3). 429–39 10.1088/0967-3334/35/3/429.

Saif Nalband is pursing Ph.D from department of Electrical Electronics & Engineering (EEE), Birla Institute of Technology and Science, Pilani, K.K Birla Goa Campus, India. Signal processing, biomedical signal processing and machine learning are the his research area of interest.

C.A. Valliappan holds a Bachelors degree in Electrical Electronics & Engineering from Birla Institute of Technology and Science, Pilani, K. K Birla Goa Campus, India. He has been working in the area of machine learning and biomedical signal processing. He is presently working as research assistance in Indian Institute of Science, Bangalore.

A.Amalin Prince completed his Ph.D from Birla Institute of Technology and Science, Pilani, Rajasthan, India in 2011. He is currently working as Assistant Professor in the department of Electrical Electronics & Engineering, Birla Institute of Technology and Science, Pilani, K. K Birla Goa Campus, India. His area of research includes VLSI architecture design, embedded system, and VLSI and FPGA signal processing.

Anita Agrawal completed her Ph.D from Government College of Engineering, Amravati, India in 2009. She has been working as Assistant Professor in the department of Electrical Electronics & Engineering, Birla Institute of Technology and Science, Pilani, K. K Birla Goa Campus, India. Her research interest lies in microelectronics, embedded system, medical image processing and signal processing.

Please cite this article as: S. Nalband et al., Time-frequency based feature extraction for the analysis of vibroarthographic signals, Computers and Electrical Engineering (2018), https://doi.org/10.1016/j.compeleceng.2018.02.046